Medical Physics 386:
The Physics of Medical Imaging 1
X-ray Imaging Notes

(Last updated: April 11, 2018)

1 Introduction

There are many different imaging modalities in the radiology department— mammography, computed radiography, digital radiography, fluoroscopy, computed tomography (CT), magnetic resonance imaging (MRI), positron-emission tomography (PET), single-photon emission tomography (SPECT), ultrasound, and more. Why are there so many modalities? Because no single modality is optimal for the wide variety of imaging tasks that arise when we try to diagnose disease. Each imaging task has different imaging requirements, so no single modality can be used for all tasks.

A major goal of an imaging medical physicist is to choose and optimize the imaging modality that maximizes the diagnostic content of the image while minimizing cost. This is not a simple task—diagnostic content depends on each specific task, and cost depends on the equipment price, the number of patients that can be imaged per unit time, the radiologists interpretation time, the cost of the exam to the patient, the risks to the patient, the consequences of a false negative exam, the cost of a false positive exam, and more.

One way to understand a medical physicist's task is to examine the relationship between cost, image quality, and diagnostic accuracy. If we assume that there is a monotonic relationship between image quality and diagnostic accuracy (Figure XXX), and if we assume that there is a similar relationship between image quality and cost (Figure XXX), then

In this part of the course, you will learn how to quantify image quality and how it is affected by various acquisition parameters. First, we will review the mathematics required and discuss common image quality metrics. Second, we will discuss x-ray imaging physics and learn how to optimize x-ray imaging systems using the previously developed metrics. Finally, we will discuss the interpretation of the x-ray images and how our interpretation fits into the broader context.

These notes draw heavily from...

Our main reference will be [1].

2 X-ray Imaging

2.1 Basics

We can create an x-ray imaging system by assembling an x-ray **source**, an **object**, and a **detector**. In this section, we will give a brief review of x-ray production, the relevant interactions that take place along the imaging chain, and we will conclude with a basic imaging model.

2.1.1 Sources and Interactions

Brief intro to x-ray production (tubes, anodes, kVp, mA, fluence, etc.)

Brief review of interactions in x-ray energy regime, definition of primary vs. scatter, etc.

2.1.2 Basic Imaging Model

Figure 1 shows a simple example of an x-ray imaging system—we place an x-ray fluence $\boldsymbol{\phi}_0$ incident on an object with two attenuation coefficients μ_1 and μ_2. Note that we use bold symbols to indicate random variables. X-rays

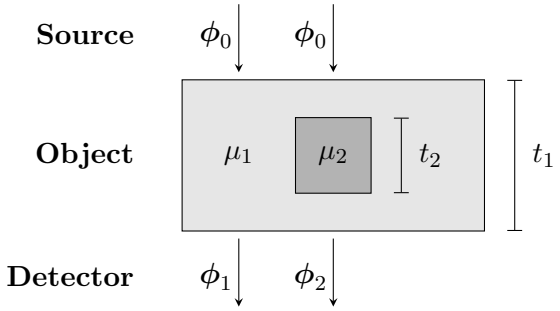

Figure 1: Simplified x-ray imaging schematic. A collimated beam of x-rays with fluence $\boldsymbol{\phi}_o$ is incident on an object with two attenuation coefficients. A detector measures the output fluences $\boldsymbol{\phi}_{1,2}$.

are attenuated as they pass through the object so the exit fluences are related to the input fluence by

$$\boldsymbol{\phi}_1 = \boldsymbol{\phi}_0 e^{-\mu_1 t_1} \tag{2.1}$$

$$\boldsymbol{\phi}_2 = \boldsymbol{\phi}_0 e^{-\mu_1 (t_1 - t_2) - \mu_2 t_2}. \tag{2.2}$$

When we place a detector in the path of the exit beam we create an image of the object.

We will examine more realistic sources and detectors in later sections, but the simple example in Figure 1 is sufficient for us to model image quality in x-ray imaging systems.

2.2 Rose Model

Suppose that we'd like to detect the presence or absence of the small object with attenuation μ_2 in Figure 1 with our imaging system. How well can we perform this task? What conditions do we need to meet to confidently say that the object is present or absent? How should we design our imaging system to meet these conditions? The Rose model supplies answers to these questions and gives us a solid framework for understanding image quality.

First, we define the **signal** S as the mean number of photons blocked by the object

$$S \equiv A(\mathrm{E}\{\boldsymbol{\phi}_1\} - \mathrm{E}\{\boldsymbol{\phi}_2\}) = A\Delta\phi \tag{2.3}$$

where A is the cross sectional area of the object, $\mathrm{E}\{\cdot\}$ denotes the expectation value, ϕ is the x-ray fluence in units of photons per unit area, and $\Delta\phi \equiv \mathrm{E}\{\boldsymbol{\phi}_1\} - \mathrm{E}\{\boldsymbol{\phi}_2\}$. This may seem like a peculiar way to define the signal—shouldn't the signal be the measured intensity difference between areas with and without the object? The reason for our definition is that it captures the role of object size in detectability. Intuitively, larger objects are easier to detect, so our definition of signal should reflect this.

Next, we consider the **noise** N that corrupts our signal. Note that in signal-to-noise ratio discussions the word "noise" usually refers to the standard deviation of a random variable. We will use this meaning. In general the word "noise" refers to any random or unwanted signals.

We define the noise as the standard deviation of the number of photons detected in an area the size of the object when the object is absent.

$$N \equiv \sqrt{\mathrm{Var}\{A\boldsymbol{\phi}_1\}}. \tag{2.4}$$

$A\boldsymbol{\phi}_1$ is a Poisson-distributed random variable, so its variance is identical to its mean

$$N = \sqrt{\mathrm{E}\{A\boldsymbol{\phi}_1\}} \tag{2.5}$$

$$N = \sqrt{A\mathrm{E}\{\boldsymbol{\phi}_1\}}. \tag{2.6}$$

Finally, the signal-to-noise ratio is given by

$$\mathrm{SNR} \equiv \frac{S}{N} = \frac{A\Delta\phi}{\sqrt{AE\{\boldsymbol{\phi}_1\}}} \tag{2.7}$$

where C is the radiation contrast:

$$C = \frac{\Delta\phi}{\bar{\phi}} \tag{2.8}$$

This is the SNR for an ideal detector where we've assumed that there is

- complete absorption of incident quanta
- no added noise
- no loss of spatial resolution (i.e., no blurring)

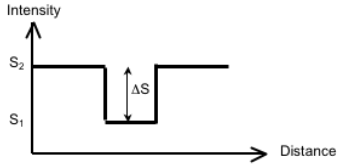

Figure 2: Test

2.3 Linear Systems Model

In this section, we aim to devise a mathematical model to describe transmission radiography. Specifically, we would like to use linear systems theory to describe the final radiographic image as a convolution of the object with a point spread function (PSF) contributed by both the x-ray source and the detector.

To begin, we consider a simplified geometric representation of an x-ray system, shown in Figure 3:

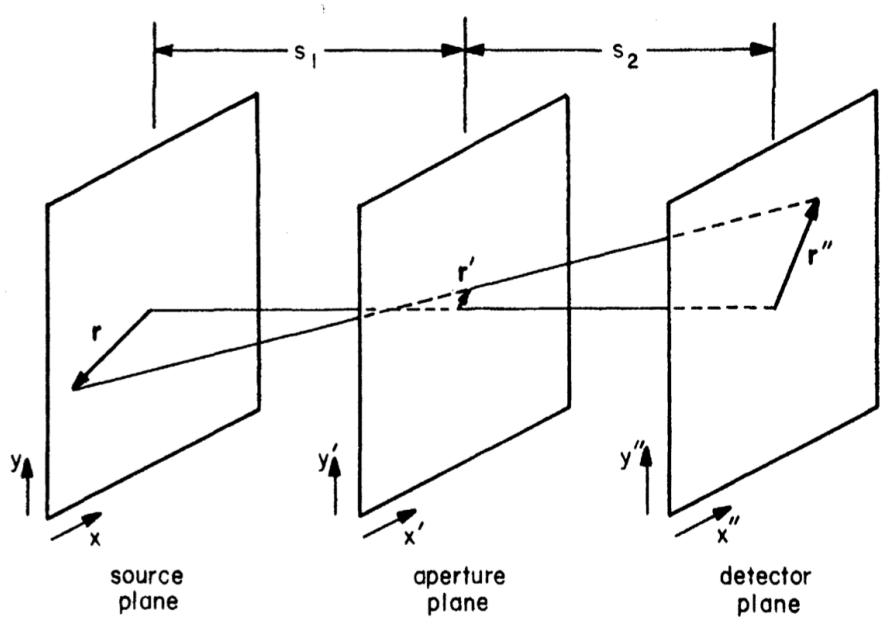

Figure 3: Simplified geometry of a radiographic imaging system. Note: we will refer to the central plane as the "object plane," not "aperture plane," as it appears here.

X-rays are generated at the anode of an x-ray tube, located in the **source plane** (with coordinate $\boldsymbol{r}$). They then pass through the **object plane** (with coordinate $\boldsymbol{r}'$), before being detected at the **detector plane** (with coordinate $\boldsymbol{r}''$). The distance between the source and object planes is s_1, and the distance between the object and detector planes is s_2. Clearly, there are a number of idealizations in this setup. We model the 3D anode and 3D object as 2D planes, and assume that all three planes are parallel. Regardless, we can still draw important insights from this simplified model.

2.3.1 The Source

We describe the source by an *emission function* $f(\boldsymbol{r})$, where $\boldsymbol{r}$ is the two-dimensional vector in the source plane. The emisison function has units of fluence rate: (photons / unit time $\cdot$ unit area). Thus, the quantity $f(\boldsymbol{r})d^2r$ is the *mean* number of photons per unit time emitted into all space from an elemental area d^2r located at the point $\boldsymbol{r}$. Note that this introduces another assumption that the source emits photons isotropically. In fact, bremsstrahlung photons have a definite preferred orientation which depends on electron energy, angle of electron incidence, and target material.

2.3.2 The Detector

Now, let us consider an elemental detector of area $d^2\boldsymbol{r}''$, where $\boldsymbol{r}''$ is the two-dimensional position vector in the detector plane. We can calculate the solid angle $d\Omega$ subtended by the elemental detector area from the source

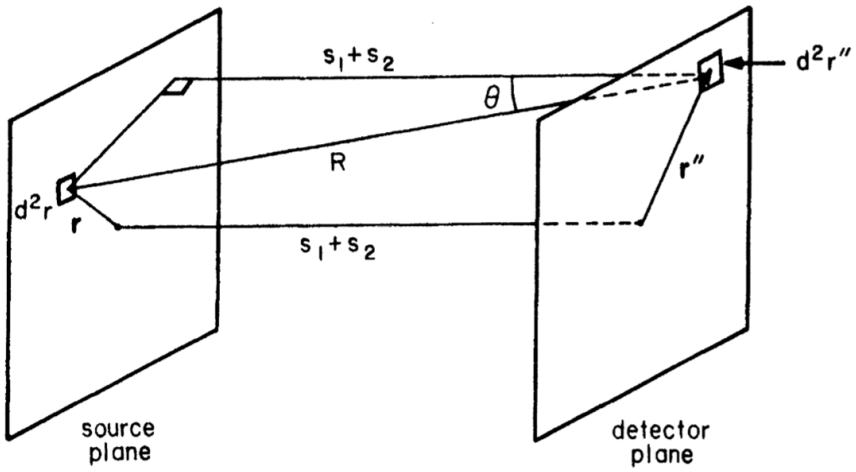

Figure 4: Diagram for solid-angle calculation.

as:

$$d\boldsymbol{\Omega} = \frac{d^2\boldsymbol{r}'' \cdot \cos\theta}{R^2}, \tag{2.9}$$

where R is the distance from the source element to the detector element and θ is the angle between the normal to the detector surface and the line of sight from source to detector, as shown in Figure 4. From simple geometry, we know that

$$R = (s_1 + s_2)/\cos\theta, \tag{2.10}$$

so we can rewrite Equation 2.9 as

$$d\boldsymbol{\Omega} = \frac{\cos^3\theta}{(s_1 + s_2)^2} d^2\boldsymbol{r}''. \tag{2.11}$$

Since a full sphere subtends 4π steradians, the detector element would intercept a fraction $d\boldsymbol{\Omega}/4\pi$ of the radiation emitted from any source element in the absence of absorbing material in between the source and detector planes. In this case, the mean number of photons per unit time (1) emitted by the area element $d^2\boldsymbol{r}$ in the source plane and (2) intercepted by the area element $d^2\boldsymbol{r}''$ in the detector plane would be

$$f(\boldsymbol{r}) d^2\boldsymbol{r} \frac{d\boldsymbol{\Omega}}{4\pi} = f(\boldsymbol{r}) \frac{\cos^3\theta}{4\pi(s_1 + s_2)^2} d^2\boldsymbol{r} d^2\boldsymbol{r}''. \tag{2.12}$$

For now, we are assuming an ideal, continuous detector that detects all photons that intercept it. We will lift this restriction shortly; in general, we will see that the detector should be considered an integral part of the imaging system.

2.3.3 The Object Plane

We now consider the effect of the object. We introduce another restriction that we are only dealing with *primary* x-rays; we will discuss the effect of scattered radiation later. A ray emanating from point $\boldsymbol{r}$ and striking the detector at point $\boldsymbol{r}''$ will have passed through the object plane at point $\boldsymbol{r}'$. We define $g(\boldsymbol{r}')$ as the transmittance,

or the fraction of photons that pass through the object plane at point $\boldsymbol{r}'$.

We are now in a position to write down an expression for $h(\boldsymbol{r}'')$, the density of detected photons, such that $h(\boldsymbol{r}'')d^2\boldsymbol{r}''$ is the mean number of photons intercepted by the detector area $d^2\boldsymbol{r}''$ in a time T. We are not interested in where exactly in the source the photons come from, so we integrate over the entire source plane:

$$h(\boldsymbol{r}'')d^2\boldsymbol{r}'' = \frac{Td^2\boldsymbol{r}''}{4\pi(s_1+s_2)^2}\int_{\text{source}} d^2\boldsymbol{r}\,\cos^3\theta f(\boldsymbol{r})g(\boldsymbol{r}'). \tag{2.13}$$

$h(\boldsymbol{r}'')$ has dimensions of fluence (photons per unit area), though we refer to $h(\boldsymbol{r}'')$ as a *photon density* instead, as that term is more appropriate to a static pattern of recorded photons.

Looking closely at the geometry of Figure 3, we see that

$$\frac{\boldsymbol{r}'-\boldsymbol{r}}{s_1} = \frac{\boldsymbol{r}''-\boldsymbol{r}'}{s_2}, \tag{2.14}$$

or, equivalently:

$$\boldsymbol{r}' = \frac{s_2}{s_1+s_2}\boldsymbol{r} + \frac{s_1}{s_1+s_2}\boldsymbol{r}'' = a\boldsymbol{r}'' + b\boldsymbol{r}, \tag{2.15}$$

where

$$a = \frac{s_1}{s_1+s_2} \qquad\qquad b = \frac{s_2}{s_1+s_2} = 1-a, \tag{2.16}$$

and we have eliminated the vector $\boldsymbol{r}'$. Note that Equations 2.14 and 2.15 describe 2D (not 3D!) vector subtractions in the parallel (x,y) and (x',y') planes. The 3D distance R would be written

$$R = \sqrt{|\boldsymbol{r}-\boldsymbol{r}''|^2 + (s_1+s_2)^2}. \tag{2.17}$$

With this simplification, we can rewrite Equation 2.13 without the use of $\boldsymbol{r}'$ as

$$h(\boldsymbol{r}'')d^2\boldsymbol{r}'' = Cd^2\boldsymbol{r}''\int_{\text{source}} d^2\boldsymbol{r}\,\cos^3\theta f(\boldsymbol{r})g(a\boldsymbol{r}''+b\boldsymbol{r}), \tag{2.18}$$

where

$$C = \frac{T}{4\pi(s_1+s_2)^2}. \tag{2.19}$$

We are generally interested in systems where s_1+s_2 is large compared to $|\boldsymbol{r}|$ or $|\boldsymbol{r}''|$. We can thus make the approximation $\theta \approx 0$ and $\cos^3\theta \approx 1$. Dropping the $d^2\boldsymbol{r}''$ factor from both sides, this leaves us with our final model for the density of detected photons:

$$h(\boldsymbol{r}'') \approx C\int_{source} d^2\boldsymbol{r}\, f(\boldsymbol{r})g(a\boldsymbol{r}''+b\boldsymbol{r}). \tag{2.20}$$

It is important to keep track of the various assumptions we used to build this model. To summarize, we assume:

- we have a 2D, planar, isotropic source that is far from the detector plane ($\theta \approx 0$)

- we have a 2D planar object that does not introduce scattered radiation
- we have an ideal detector that perfectly detects every photon it encounters

2.3.4 Reduction to a Convolution

Equation 2.20 is starting to resemble a convolution integral. To exploit this resemblance, we define a new variable $\boldsymbol{r}_0''$, given by

$$\boldsymbol{r}_0'' = \frac{s_2}{s_1}\boldsymbol{r} = -\frac{b}{a}\boldsymbol{r}. \tag{2.21}$$

Multiplication of $\boldsymbol{r}$ by $-b/a$ is equivalent to projecting it through a point in the object plane to the image plane, as illustrated in Figure 5.

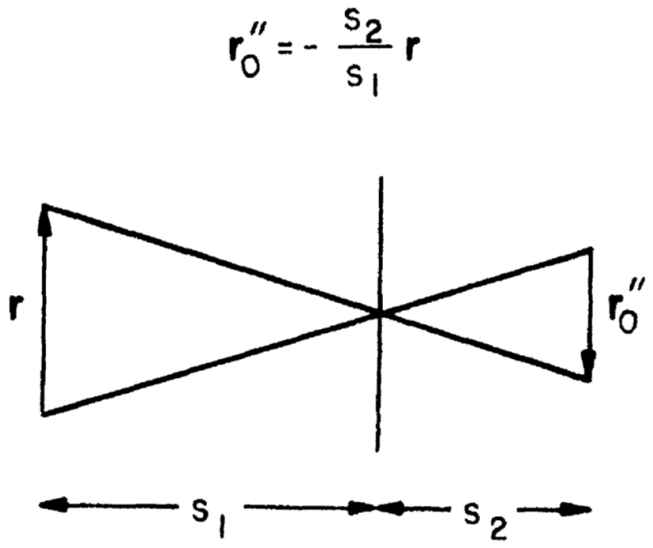

Figure 5: Illustration of $\boldsymbol{r}_0''$.

We can use $\boldsymbol{r}_0''$ to define scaled versions of f (the source emittance) and g (the object transmittance). We define these scaled functions as $\tilde{f}$ and $\tilde{g}$, respectively:

$$\tilde{f}(\boldsymbol{r}_0'') = f(\boldsymbol{r}) = f\left(-\frac{a}{b}\boldsymbol{r}_0''\right) \tag{2.22}$$

$$\tilde{g}(\boldsymbol{r}_0'') = g(a\boldsymbol{r}_0''). \tag{2.23}$$

The tilde thus indicates *projection of the initial functions onto the image plane.* We can rewrite g in terms of these new variables:

$$g(a\boldsymbol{r}'' + b\boldsymbol{r}) = g(a\boldsymbol{r}'' - a\boldsymbol{r}_0'') = \tilde{g}(\boldsymbol{r}'' - \boldsymbol{r}_0''), \tag{2.24}$$

which leads to a final form for $h(\boldsymbol{r}'')$:

$$\begin{aligned} h(\boldsymbol{r}'') &= \left(\frac{a}{b}\right)^2 C \int_\infty d^2\boldsymbol{r}_0'' \tilde{f}(\boldsymbol{r}_0'')\tilde{g}(\boldsymbol{r}'' - \boldsymbol{r}_0'') \\ &= \left(\frac{a}{b}\right)^2 C \tilde{f}(\boldsymbol{r}'') ** \tilde{g}(\boldsymbol{r}'') \end{aligned} \tag{2.25}$$

where the ∞ subscript in the integral indicates integration over the entire 2D detector plane. We have thus achieved our goal and described the detected photon density as the output of a 2D linear system with input $\tilde{f}$ and kernel proportional to $\tilde{g}$ (or equivalently, an input $\tilde{g}$ and kernel proportional to $\tilde{f}$). As with any linear system, a frequency-domain description is very useful:

$$\mathscr{F}_2\left\{h(\boldsymbol{r}'')\right\} = H(\boldsymbol{\rho}'') = (a/b)^2 C\tilde{F}(\boldsymbol{\rho}'')\tilde{G}(\boldsymbol{\rho}), \tag{2.26}$$

where $\boldsymbol{\rho}''$ is the spatial frequency vector conjugate to $\boldsymbol{r}''$ in the image plane. Recall the scaling relation for an nD Fourier transform:

$$\mathscr{F}_N\left\{f(\boldsymbol{r}/b)\right\} = |b|^N F(b\boldsymbol{\rho}). \tag{2.27}$$

We can use this to evaluate the right side of Equation 2.26 in terms of the original source and transmission functions f and g:

$$\tilde{F}(\boldsymbol{\rho}'') = \mathscr{F}_2\left\{f(-a\boldsymbol{r}''/b)\right\} = (b/a)^2 F(-b\boldsymbol{\rho}''/a) \tag{2.28}$$

$$\tilde{G}(\boldsymbol{\rho}'') = \mathscr{F}_2\left\{g(a\boldsymbol{r}'')\right\} = (1/a)^2 G(\boldsymbol{\rho}''/a). \tag{2.29}$$

Our final result is then

$$H(\boldsymbol{\rho}'') = (C/a^2)F(-b\boldsymbol{\rho}''/a)G(\boldsymbol{\rho}''/a). \tag{2.30}$$

Recall that the double-primed coordinate represent the frequency vector in the image plane. We can also express Equation 2.30 in the object ($\boldsymbol{\rho}'$) and source ($\boldsymbol{\rho}$) planes:

$$H(a\boldsymbol{\rho}') = (C/a^2)F(-b\boldsymbol{\rho}')G(\boldsymbol{\rho}') \tag{2.31}$$

$$H(-a\boldsymbol{\rho}/b) = (C/a^2)F(\boldsymbol{\rho})G(-\boldsymbol{\rho}/b). \tag{2.32}$$

2.3.5 Effect of focal spot

The perhaps non-intuitive result of this analysis is that the x-ray source plays such an important role in the imaging chain. We have shown that the detected image can be modeled as a convolution of the object with the x-ray source – the source is thus always "in" the image, in a certain sense. We would like to characterize this effect in more detail.

We can model the x-ray source as a "focal spot," a uniform, emissive disk of diameter d_{fs}, so the emission function is

$$f(\boldsymbol{r}) = f_0 \text{ circ}\left(\frac{2r}{d_{fs}}\right), \tag{2.33}$$

where f_0 is the emission density (photons per unit area per unit time) within the disk region (see Figure 6). Recall that the "circ" function is defined as:

$$\text{circ}(r) = \begin{cases} 1 & r \leq 1 \\ 0 & \text{else} \end{cases}. \tag{2.34}$$

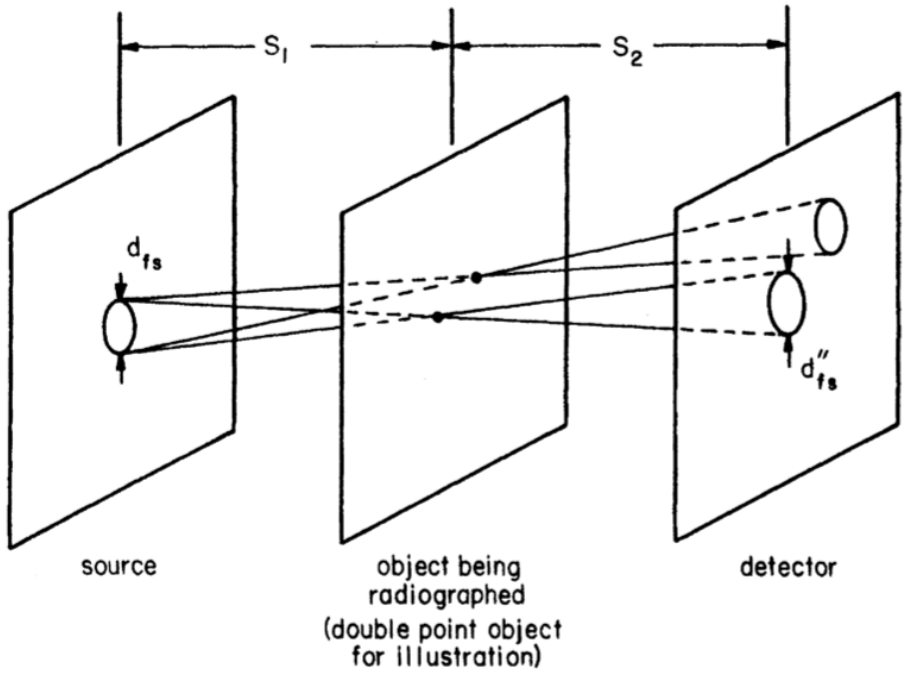

Figure 6: Diagram illustrating the calculation of the point spread function for transmission radiography with a disklike focal spot.

To find the PSF of the system, we consider a point object input described by

$$g(\boldsymbol{r}') = \delta(\boldsymbol{r}' - \boldsymbol{r}'_1), \tag{2.35}$$

where $\boldsymbol{r}'_1$ is the location of the point in the object plane. The notion of a "point" transmission might seem counterintuitive – we are describing a hypothetical object that becomes "infinitely transmissive" over an infinitesimal area. You might consider a pinhole aperture with area approaching zero while the exposure time is increased proportionally.

The PSF is just the image of a point source measured in the detector plane – i.e., the pinhole image of the focal spot. Substituting Equations 2.33 and 2.35 into 2.20, we find

$$\begin{aligned} h(\boldsymbol{r}'') &= C \int_{source} d^2\boldsymbol{r} f_0 \ \text{circ}\left(\frac{2r}{d_{fs}}\right) \delta(a\boldsymbol{r}'' + b\boldsymbol{r} - \boldsymbol{r}') \\ &= \left(\frac{C}{b^2}\right) f_0 \ \text{circ}\left[\frac{2|a\boldsymbol{r}'' - \boldsymbol{r}'_1|}{bd_{fs}}\right] \\ &= \left(\frac{C}{b^2}\right) f_0 \ \text{circ}\left[\frac{2|\boldsymbol{r}'' - (\boldsymbol{r}'_1/a)|}{bd_{fs}/a}\right], \end{aligned} \tag{2.36}$$

where we have made use of the sifting property of delta functions. This equation describes a uniform disk image of diameter d''_{fs}, given by

$$d''_{fs} = \frac{b}{a} d_{fs} = \frac{s_2}{s_1} d_{fs}. \tag{2.37}$$

The disk is centered at $\boldsymbol{r}'' = \boldsymbol{r}'_1/a = \boldsymbol{r}'_1(s_1 + s_2)/s_1$, the magnification m_t is therefore $(s_1 + s_2)/s_1$. Note that m_t is always a positive number greater than 1.

To completely specify the PSF we must also include the effects of the image detector, which we have so far neglected. An ideal detector would produce output directly proportional to $h(\boldsymbol{r''})$. Real detectors, however, further degrade the image and must be treated as independent linear systems. Cascaded linear systems are easiest to deal with in the frequency domain, so we consider the input of the *detector* system to be $H(\boldsymbol{\rho}'')$, the Fourier transform of $h(\boldsymbol{r}'')$. We denote the transfer function of the detector as $D(\boldsymbol{\rho}'')$, so the detector output is just $D(\boldsymbol{\rho}'')H(\boldsymbol{\rho}'')$. Using Equation 2.30, we can write this as

$$D(\boldsymbol{\rho}'')H(\boldsymbol{\rho}'') = (C/a^2)D(\boldsymbol{\rho}'')F(-b\boldsymbol{\rho}''/a)G(\boldsymbol{\rho}''/a). \tag{2.38}$$

This describes the transfer of spatial frequencies $G(\boldsymbol{\rho}''/a)$, the object function scaled into the detector plane. We are *actually* interested in how the spatial frequencies of the object in the *object plane* (i.e., with no scaling) are affected by the system, so we let $\boldsymbol{\rho}' = \boldsymbol{\rho}''/a$ and rewrite our result as

$$D(a\boldsymbol{\rho}')H(a\boldsymbol{\rho}') = (C/a^2)D(a\boldsymbol{\rho}')F(-b\boldsymbol{\rho}')G(\boldsymbol{\rho}'). \tag{2.39}$$

Note that $G(\boldsymbol{\rho}')$ now appears on the right side with no scaling. The overall transfer function of the system for spatial frequencies in the object plane is thus given by

$$TF_{tot}(\boldsymbol{\rho}') = P_{tot}(\boldsymbol{\rho}') = (C/a^2)D(a\boldsymbol{\rho}')F(-b\boldsymbol{\rho}'), \tag{2.40}$$

which we can write in the spatial domain as

$$\mathrm{PSF}_{tot}(\boldsymbol{r}') = p_{tot}(\boldsymbol{r}') = (C/a^2)\mathscr{F}_2^{-1}\left\{D(a\boldsymbol{\rho}')F(-b\boldsymbol{\rho}')\right\} \tag{2.41}$$

$$= p_{fs}(\boldsymbol{r}') ** p_{det}(\boldsymbol{r}'), \tag{2.42}$$

where $p_{fs}(\boldsymbol{r}')$ is the PSF due to the focal spot alone:

$$p_{fs}(\boldsymbol{r}') = (C/a^2)\mathscr{F}_2^{-1}\left\{F(-b\boldsymbol{\rho})\right\} = \left(\frac{C}{a^2b^2}\right) f\left(-\boldsymbol{r}'/b\right), \tag{2.43}$$

and $p_{det}(\boldsymbol{r}')$ is the PSF due to the detector:

$$p_{det}(\boldsymbol{r}') = \mathscr{F}_2^{-1}\left\{D(a\boldsymbol{\rho}')\right\} = (1/a^2)d\left(\boldsymbol{r}'/a\right). \tag{2.44}$$

2.3.6 Design Considerations

We can now discuss how to use our results from the linear systems model to optimize our imaging system design. Specifically, we see that there is an optimum magnification even if there is no limitation imposed by

the finite detector size. Recall that the magnification is given by

$$m_t = \frac{s_1 + s_2}{s_1} = \frac{1}{a} = \frac{1}{1-b}. \tag{2.45}$$

Equivalently, we see that

$$b = 1 - \frac{1}{m_t} = \frac{m_t - 1}{m_t}. \tag{2.46}$$

Applying these results to Equations 2.43 and 2.44, we see that

$$p_{fs}(\boldsymbol{r}') \propto f\left(\frac{-m_t \boldsymbol{r}'}{m_t - 1}\right) \tag{2.47}$$

$$p_{det}(\boldsymbol{r}') \propto d(m_t \boldsymbol{r}') \tag{2.48}$$

The width of $p_{fs}(\boldsymbol{r}')$ is smallest when the coefficient of $\boldsymbol{r}'$ of Equation 2.47 is the largest, which occurs when $m_t = 1$. Blurring from the focal spot is thus minimized for "contact" imaging ($s_2 = 0$), when the detector is in direct contact with the object being imaged, and there is no magnification. We see from Equation 2.48, however, that a large magnification is needed to minimize blurring from the detector.

To optimize the choice of magnification, then, we can model the PSFs from the focal spot and detector as Gaussians. Recall that the Fourier transform of a Gaussian function is another Gaussian function. In the frequency domain then, we will assume that

$$D(\boldsymbol{\rho}'') \propto \exp\left[-\pi\left(\boldsymbol{\rho}''/\rho_d''\right)^2\right] \tag{2.49}$$

$$F(\boldsymbol{\rho}) \propto \exp\left[-\pi\left(\boldsymbol{\rho}/\rho_f\right)^2\right], \tag{2.50}$$

where ρ_d'' and ρ_f are characteristic widths of the MTF of the detector and focal spot, respectively. We find the overall MTF from Equation 2.40,

$$\mathrm{MTF}_{tot} = \frac{|P_{tot}(\boldsymbol{\rho}')|}{P_{tot}(0)} \propto \exp\left[-\pi(a\boldsymbol{\rho}'/\rho_d'')^2\right] \exp\left[-\pi(b\boldsymbol{\rho}'/\rho_f'')^2\right]. \tag{2.51}$$

From Equations 2.45 and 2.46, this can be written as

$$\mathrm{MTF}_{tot} = \exp\left[-\pi\boldsymbol{\rho}'\left(\frac{1}{(m_t\rho_d'')^2} + \frac{(m_t-1)^2}{(m_t\rho_f)^2}\right)\right]. \tag{2.52}$$

The width of MTF_{tot} will be an extremum if

$$\frac{d}{dm_t}\left[\frac{1}{(m_t\rho_d'')^2} + \frac{(m_t-1)^2}{(m_t\rho_f)^2}\right] = 0, \tag{2.53}$$

which has the solution

$$m_t^{opt} = 1 + \left(\frac{p_f}{p_d}\right)^2. \tag{2.54}$$

We are interested in two limits of Equation 2.54. If we have a very large focal spot ($\rho_f \to 0$), then $m_t^{opt} = 1$,

which, as we have already discussed, indicates contact imaging. On the other hand, if our detector is very poor ($\rho_d'' \to 0$), we require a large magnification. In other words, we can tolerate having a large focal spot by performing contact imaging, at the cost of having no magnification. This is generally what occurs, as the focal spot is often a more dominant contribution to the system PSF than the detector.

Note: this discussion on linear systems theory was adapted from Chapter 4 in Barrett [1]. Please read through the rest of that chapter for a more detailed analysis and insight into further design considerations.

3 X-ray Detectors

3.1 Ideal Detector

3.2 Detector Metrics

3.2.1 SNR

3.2.2 DQE

3.2.3 NEQ

3.3 Analog Detectors

3.3.1 Film structure

3.3.2 Optical density / H&D Curve

3.3.3 Important Film properties (speed, etc.)

3.3.4 Intensifying Screen

3.3.5 DQE of film

3.3.6 MTF of film

3.3.7 Physics modeling of Film (Ag grain density, etc)

3.3.8 Model of intensifying Screen PSF

3.3.9 MTF of Screen-Film

3.4 Digital Detectors

3.4.1 Intro

3.4.2 DQE

3.5 Comparison

3.5.1 Detectors

An ideal x-ray detector converts an x-ray image into a visible image without altering it. In this section we will review the major types of x-ray detectors and examine how they fail to be ideal.

The first task of any x-ray detector is to absorb all incident x-rays—a detector should not let any x-rays pass through. The fraction of incident x-rays that interact in the detector, η, is called the quantum detection efficiency. The quantum detection efficiency is related to the linear attenuation coefficient of the x-ray detector, μ, and the thickness of the detector t by

$$\eta = 1 - e^{-\mu t}. \tag{3.1}$$

An ideal detector will stop all x-rays, so we would like μt to be as large as possible. Therefore, an x-ray detector should be thick and made of a material with high atomic number and high physical density. If the quantum

detection efficiency is less than one, then the detector's SNR will be reduced by $\sqrt{\eta}$ and Eq. XXX becomes

$$\text{SNR} = C\sqrt{\eta A\bar{\phi}}. \tag{3.2}$$

Recall from the Rose model that we need to an SNR of approximately 5 to detect a signal on a background. This means that reducing the quantum efficiency will require us to increase the incident x-ray fluence to maintain a fixed SNR. Increasing the photon fluence will increase the dose to the patient, so clearly quantum efficiency is an important consideration for all detectors.

Analog Detectors

Analog images are acquired and displayed on film. Film consists of a plastic base coated with a gelatin binder that contains light-sensitive silver halide crystals. Figures 7 and 8 show schematic and scanning electron micrograph views of film.

When a photon hits a (transparent) silver halide crystal, a photochemical reaction occurs that creates two (opaque) metallic silver atoms. Under typical conditions the number of metallic silver atoms is far too small for the film to become visibly opaque to human eyes, but the film now contains a latent image in the form of silver atoms within silver halide grains. To make the image visible, we need to "amplify" the number of metallic silver atoms in each grain using a *developer solution*, then remove the unexposed silver halide crystals using a *fixing solution*. The result is a *photographic negative* that is dark (lots of metallic silver) in regions that have been exposed and light in regions that have not been exposed. In x-ray imaging the photographic negative is used directly, but in photographic imaging you need to invert the film brightness by projecting light through the negative, imaging the result on film, then repeating the development process. See [1, 2] for a more detailed discussion of the film development process.

For an x-ray film with a thin coat of silver halide grains, the grain size determines the spatial resolution. Film grains are approximately 0.2-2 μm in diameter which gives us a sense of the smallest resolvable feature. For comparison a typical 2018 scientific CCD has a pixel width of 6 μm and an iPhone X display has a pixel width of 55 μm. Film has unmatched spatial resolution even in 2018.

Only a few percent of incident x-rays interact as they pass through film. Because quantum efficiency is so important for medical imaging, most medical x-ray film uses a photographic emulsion coating on both sides of the plastic base. We could increase the thickness of the emulsion layers to improve quantum efficiency further, but this would reduce spatial resolution and make developing the film more difficult.

We can improve the quantum efficiency of film by placing a *fluorescence screen* directly on the film. Fluorescence screens have a high attenuation coefficient and contain an x-ray phosphor that converts incident x-rays into many visible (plus infrared and ultraviolet) photons. These visible photons expose the film and the film can be developed normally. Unfortunately, the visible photons do not travel straight to the film along their generating x-ray's path—they spread out before they reach the film. This means that using a fluorescence screen improves quantum efficiency at the expense of spatial resolution. This type of detector is often called an *indirect analog* detector because it indirectly detects the incident x-rays.

The input to a film detector is the x-ray exposure measured in coulombs per kilogram (C/kg) or röntgen (R). The output of a film detector is usually measured with a unitless property called optical density (OD). If a thin beam of light with intensity I_0 hits the film and the transmitted beam has intensity I, then the optical

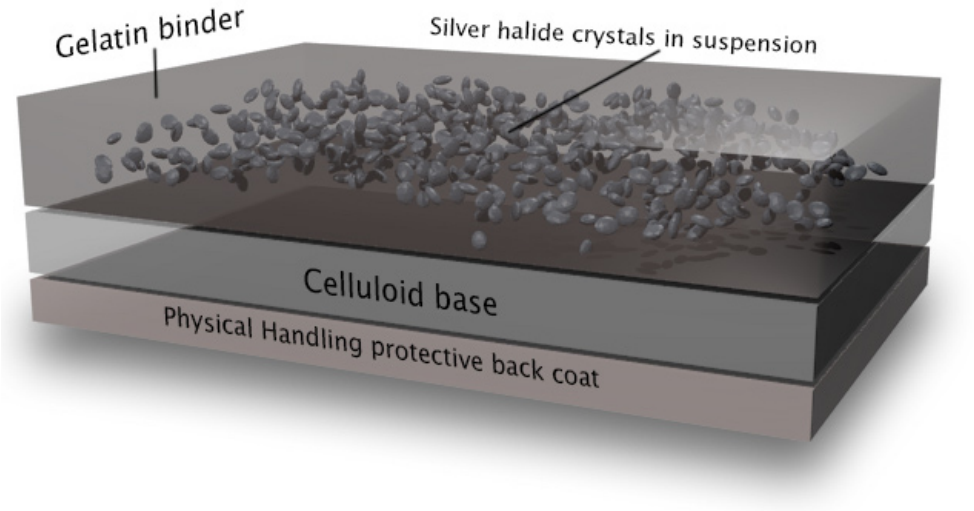

Figure 7: Schematic view of photographic film. [2]

density of the film at that point is defined as

$$\mathrm{OD} = -\ln\left(\frac{I}{I_0}\right). \tag{3.3}$$

A high OD means that the film is opaque which corresponds to a high x-ray exposure. The relationship between x-ray exposure (input) and optical density (output) is often called the *characteristic* curve, the *Hurter-Driffield* curve, or the D—$\log E$ curve. An example of a characteristic curve is shown in Fig. 9. Note the often confused units on the characteristic curve—the horizontal axis uses a logarithmic exposure scale and the vertical axis uses a linear scale for optical density which is itself a logarithm of the input-output intensity ratio (see Eq. 3.3).

Let's examine the features of the characteristic curve in Fig. 9. When the film has not been exposed the optical density is not zero—even unexposed film is not completely transparent due to reflections, impurities, and thermal effects. As we start to expose the film, we begin to create metallic silver atoms. A single metallic silver atom in a grain is not enough to create a latent image though; about 4 metallic silver atoms are required in a single grain to ensure that it will be developed. This means that for low exposures the optical density will increase slowly—this is evident in the "toe" of the characteristic curve. At high exposures most of the grains in the film already have many metallic silver atoms, so increasing the exposure will not increase the optical density further—this is evident in the "shoulder" of the characteristic curve. Finally, at intermediate exposures the optical density increases linearly with the log exposure. The slope of characteristic curve is often called the *speed* of the film because it summarizes how quickly a fixed exposure rate will increase the optical density—this terminology is borrowed from photographers who will use a "fast" film in situations where they require short exposure times e.g. sports photography. See [1] chapter X for a complete derivation of film's characteristic curve.

The characteristic curve also depends on the film processing conditions which can vary significantly. The proportions of chemicals in the developer solution and the temperature will affect the shape of the characteristic curve and the speed point. Care is taken to keep the chemistry and the temperature of the developer as constant as possible.

Film's characteristic curve also depends on the exposure rate. The metallic silver atoms in each grain are

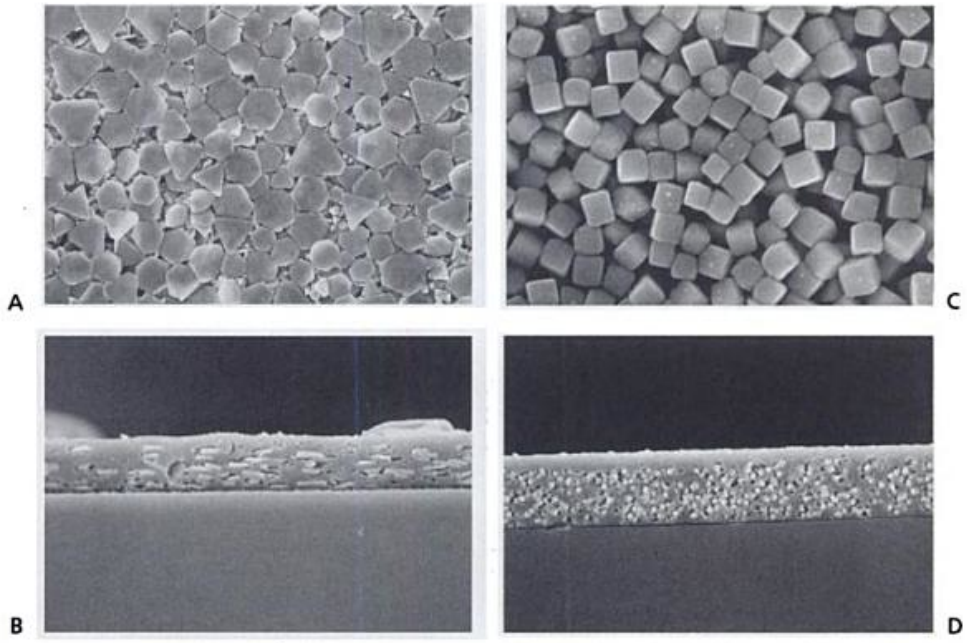

Figure 8: Scanning electron micrographs (SEM) of photographic film. **A**: A top-down SEM image of the emulsion layer of T grain emulsion. **B**: A cross section of the T grain emulsion film showing the grains in the gelatin layer supported by the polymer film base below. **C**: Cubic grain film emulsion in a top-down SEM view. **D**: Cross section of the cubic grain film. SEM courtesy of Drs. Bernard Apple and John Sabol. Citation needed.

unstable and will re-ionize back into the silver halide crystal over time. If the exposure rate is very low, then these re-ionization events can significantly reduce the number of developable grains which will reduce the OD in the final image. In other words, the characteristic curve will shift to the right for low exposure rates. This property of film is often referred to as *reciprocity law failure* or the *Schwarzschild effect* after Schwarzchild noticed the issue while imaging dim stars.

Digital Detectors

We will briefly discuss several types of digital detectors and leave the details for Patrick's lectures. The defining feature of a digital detector is that its output is a digital signal with discrete values. Digital images are usually displayed electronically, but they can be also printed on film. Thus, the acquisition of the image is separate from the display of the image and each component can be optimized separately. The input to a digital detector is exposure, and the output is a pixel value (PV). Digital systems usually respond linearly to x-ray exposure.

Indirect digital detectors use a phosphorescent screen (often CsI) coupled to a charge-couple device (CCD) camera or a think-film transistor (TFT) water. Incident x-rays are converted to visible photons in the screen which generates a signal in the CCD. Indirect digital detectors are analogous to indirect analog detectors.

Direct digital detectors use materials that produce electron-hole pairs that can be collected directly. Selenium (Se), amorphous silicon (a-Si), and cadmium zinc telluride (CZT) are common materials for direct digital detectors. An electric field is applied across the width of the detector and the electron-hole pairs follow the field lines that are perpendicular to the surface of the detector where they are collected and read out.

Photon counting detectors can measure individual x-ray interactions. Some direct digital detectors can act as photon-counting detectors. Non-photon counting detectors integrate quanta (photons or electrons) over the

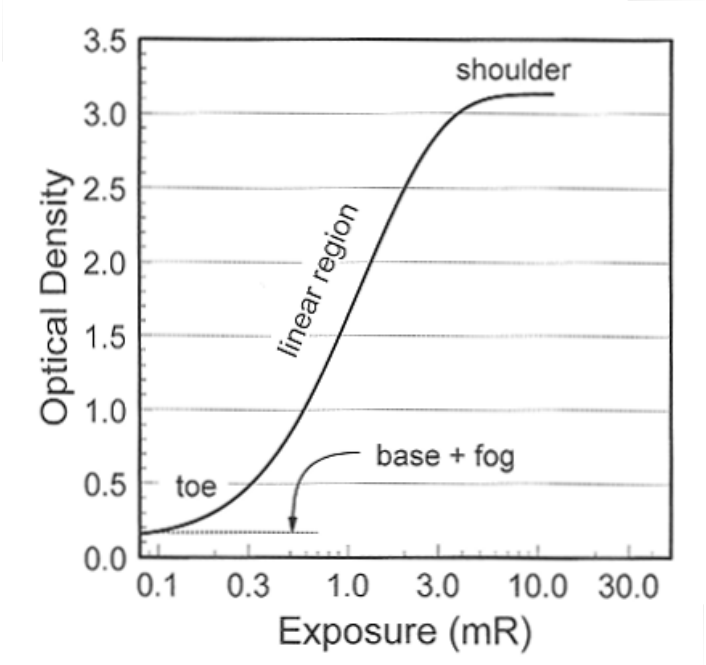

Figure 9: A characteristic curve for film. Notice the logarithmic scale on the horizontal axis and the linear scale on the vertical axis.

total exposure time of the image acquisition.

Computed radiography (CR) detectors store a latent image as electrons trapped in a phosphor screen (usually BaFCl). The electrons are subsequently read out by scanning the phosphor with a laser beam. The laser light stimulates the trapped electrons back into the conduction band where they can return back to the valence band with the emission of light. The emitted light is collected to create a digital image. These detectors use the same principle as optically stimulated luminescent dosimeters (OSLD) in radiation dosimetry.

3.5.2 *Comparison of Analog and Digital Detectors

Contrast

Speed

Latitude

Resolution

Noise

SNR

The contrast in the image incident on the detector is given (ignoring any scattered radiation) by the radiation contrast, Eq. [4]. We want to know the radiographic contrast — the contrast in the final image. To determine this, we need to know how the x-ray exposure incident on the detector is converted to a visible image. This relationship between the input exposure and the output image is given by the characteristic curve.

b. Characteristic Curve

Gives the relationship between the detector output and the exposure to the detector. For a digital detector the characteristic curve is linear. That is,

$$\mathrm{PV} = GE \tag{3.4}$$

where PV is the pixel value in the image, G is the slope of the characteristic curve and E is the incident exposure. Further:

$$\frac{\Delta E}{\bar{E}} = \frac{\Delta \mathrm{PV}}{\bar{\mathrm{PV}}} = C. \tag{3.5}$$

That is, for a digital detector, the radiographic contrast is equal to the radiation contrast and this is true for all exposure values. It is independent of the slope of the characteristic curve.

The characteristic curve for a screen-film system depends on the properties of the screen-film system and the film processing (developer) conditions.

For a screen-film system, the radiographic contrast is given by the difference in optical density, D. It depends on the radiation contrast and the slope of the H&D curve, called gamma (G). Radiographic contrast in a screen-film image is given by:

$$G = \frac{\Delta D}{\Delta(\ln E)} \tag{3.6}$$

$$\Delta D = G(\log_{10} e)\Delta(\ln E) = G(\log_{10} e)\frac{\Delta E}{\bar{E}} = CG \log_{10} e, \tag{3.7}$$

since $\phi = kE$, then $\frac{\Delta E}{\bar{E}} = \frac{\Delta \phi}{\phi} = C =$ radiation contrast.

Since the characteristic curve is not linear, the exposure to the detector is very important. The image can be properly exposed, but also under or over exposed, where the radiographic contrast will be low (because G is low). For digital system, this is not a problem (at least in terms of contrast) as illustrated below.

Effect of characteristic curve shape. Top is for screen-film, which have a non-linear response. Bottom is for a digital system with a linear response. This figure only illustrates the effect on radiographic contrast and not noise nor SNR.

c. Speed

Speed is defined as the reciprocal of the exposure required to reach a net OD of 1.0. The speed point is considered the exposure to give a properly exposed image. A fast system has high speed and slow system has low speed. Screen-film systems have an optimum exposure that must be used in order to produce a useful image.

Factors Affecting Speed 1. X-ray absorption by the screen - phosphor type (atomic number, k-edge energy) - thickness and packing density - x-ray energy - crystal size 2. Conversion Efficiency of Screen (fraction of x-ray energy converted in optical energy) - physical properties of phosphor - optical properties of screen - concentration of activator atoms - x-ray energy 3. Film Sensitivity - silver content - sensitizers - film gain size, structure, etc. 4. Matching of light emission of the screen to the spectral sensitivity of the film 5. Film processing

d. Latitude

For screen-film systems, since the curve is non-linear, the system has limited latitude. Latitude refers to the range in exposure that will produce density within the accepted range for diagnostic radiology (usually considered to be 0.25 to 2.0). Latitude does not apply to digital systems. For screen-film systems, there is a tradeoff in latitude and contrast. Generally speaking, systems with high contrast (large G) have limited latitude and vice versa.

For the image on the right, System A has higher speed and wider latitude than System B. System B has higher contrast, but limited latitude.

Wide latitude is important for imaging tasks where there are large difference in tissue types. For example a chest image requires that image display lung tissue (mostly air) and ribs (bone). Wide latitude is required to image both of these simultaneous with good contrast. With a digital detector, since the response to x-ray exposure is linear, the display of the image can be manipulated so that bone can be displayed properly and then lung tissue; or image processing can be used so that both are imaged optimally in a single image.

e. Resolution In a phosphor screen, x rays are converted to optical photons that must travel through the bulk of the screen to escape. For screens that are composed of crystals of phosphor in a binder material (turbid screen), the light is scattered multiple times as illustrated below and light can be absorbed in the screen. The light at the output of the screen is spread over a finite area, reducing spatial resolution. The scattering of light in the screen increases spatial resolution because it preferentially reduces light photons that travel a long distance. Recall that resolution can be characterized by the point spread function (psf) and the modulation transfer function (MTF). The image below gives a qualitative depiction of how the scattering of light broadens the psf and thus reduces the high frequency components of the MTF.

The spatial resolution is reduced (more spread of light) as the thickness of the screen increases. The further the distance the light needs to travel to exit the screen, the broader the psf will be. In many instances a film is sandwiched between two thinner screens rather than be used with a single thick screen. This can improve the resolution compared to using a single thick screen. It is important that the screen and film be in close contact, as any space (poor contact) will increase the area over which the light has spread.

In CsI phosphor, the crystals of CsI form long needle shaped structures. These needles act like an optical fiber reducing the lateral spread of light improving the resolution compared to turbid screens of equal thickness.

For direct digital detectors, the spatial resolution can be very high. An electric field can be placed across the photoconductor forcing the electrons to travel in direction perpendicular to the surface of the detector greatly reducing the lateral spread of the electrons.

f. X-ray Quantum Noise

The signal in a screen-film system, the signal is radiographic contrast, as given in Eq. [9]. The noise in as screen-film image is σ_D, and it is related to the noise in the x-ray image incident on the detector, σ_E.

For a uniform exposure, we can average the square of $\Delta D = D(x,y) - \bar{D}$ over an area in the image to calculate σ_D:

$$\sigma_D^2 = \frac{1}{4XY}\int_{-X}^{X}\int_{-Y}^{Y} \Delta D^2(x,y)dxdy. \tag{3.8}$$

Similar equations can be written in terms of PV and exposure to the detector, E.

$$\sigma_{\mathrm{PV}}^2 = \frac{1}{4XY}\int_{-X}^{X}\int_{-Y}^{Y} \Delta \mathrm{PV}^2(x,y)dxdy \tag{3.9}$$

$$\sigma_{\mathrm{E}}^2 = \frac{1}{4XY}\int_{-X}^{X}\int_{-Y}^{Y} \Delta \mathrm{E}^2(x,y)dxdy \tag{3.10}$$

Then by Eqs [10] and [11]"

$$\Delta D = CG\log_{10} e = G(\log_{10} e)\frac{\Delta E}{\bar{E}}, \tag{3.11}$$

but

$$E = kN \text{ and} \tag{3.12}$$

$$\sigma_E^2 = k^2\sigma_N^2 \tag{3.13}$$

where N is the number of photons, which is $N = A\phi$, where A is the cross-sectional area and ϕ is the fluence.

Eq. [14] becomes:

$$\sigma_D^2 = G^2(\log_{10}^2 e)\frac{k^2\sigma_N^2}{k^2\bar{N}^2} = G^2(\log_{10}^2 e)\frac{\sigma_N^2}{\bar{N}^2} \tag{3.14}$$

For Poisson statistics,

$$\sigma_N^2 = \bar{N} = A\bar{\phi}\text{and}\frac{\sigma_N^2}{\bar{N}^2} = \frac{1}{\bar{N}} = \frac{1}{A\bar{\phi}}. \tag{3.15}$$

Inserting Eq. [19] into [17] gives:

$$\sigma_D^2 = \frac{G^2(\log_{10}^2 e)}{A\bar{\phi}}. \tag{3.16}$$

For a digital system, PV $= GE$ and therefore

$$\Delta\text{PV} = G\Delta E. \tag{3.17}$$

Now using Eqs. [13] and [20]

$$\sigma_{PV}^2 = G^2\sigma_E^2. \tag{3.18}$$

Using Eqs [16], [17], [18] and [21]

$$\sigma_{\text{PV}}^2 = G^2k^2\sigma_N^2 = G^2k^2A\bar{\phi} \tag{3.19}$$

Note $\sigma_D^2 \propto \frac{1}{\bar{\phi}}$, but $\sigma_{\text{PV}}^2 \propto \bar{\phi}$.

Note in real imaging systems, there are other noise sources. In particular, in a screen-film system there is noise due the finite size and number of the silver grains in the developed film; and in a digital system there is electronic noise from the device that captures the light (indirect detectors) or the electrons (direct detectors). These are usually small compared to quantum noise, at low spatial frequencies. More about this in the lecture on noise.

SNR (ignoring image blurring and considering only x-ray quantum noise)

For screen-film systesms, using Eqs. [10] and [19]

$$\text{SNR}_{\text{film}} = \frac{\Delta D}{\sigma_D} = \frac{GC(\log_{10} e)}{\sqrt{\frac{G^2(\log_{10}^2 e)}{A\bar{\phi}}}} = C\sqrt{A\bar{\phi}}, \tag{3.20}$$

which is the same as Eq. [3].

For a digital system, using Eqs. [15], [20] and [22]

$$\mathrm{SNR}_{\mathrm{digital}} = \frac{\Delta \mathrm{PV}}{\sigma_{PV}} = \frac{G\Delta E}{\sqrt{G^2 k^2 A\phi}} = \frac{k\Delta N}{\sqrt{k^2 A\phi}} = \frac{A\Delta\phi}{\sqrt{A\phi}} = C\sqrt{A\bar{\phi}}, \tag{3.21}$$

which is again Eq. [3].

Non-ideal Detectors

Assume the imaging system is linear or linearizable. Further assume $w_{in}(u)$ is the input stimulus where u is an independent variable and $w_{out}(u)$ is the output response of the system. If there are two inputs, which produce two outputs, that is: $w'_{out}(u) = w'_{in}(u)$ and $w''_{out}(u) = w''in(u)$, the system is said to be linear if, when both inputs are applied together, $w_{in}(u) = w'in(u)+w''in(u)$, the output is given by: $wout(u) = w'out(u)+w''out(u)$.

For a real (non-ideal) imaging system, the input maybe localized to a location u_0, the response at the output is spread over a range of u centered on $u0$. Conversely, any point at the output will depend on input stimuli over a range of positions at the input, that is:

$$w_{out}(u) = \int_{-\infty}^{\infty} p(u, u')w_{\mathrm{in}}(u')du'$$

Let $w_{\mathrm{in}}(u) = \delta(u - u_0)$.

4 X-ray Image Quality

In this section we will introduce the basics of x-ray imaging and develop three tools that we can use to quantify image quality—contrast, resolution, and noise. We will focus on x-ray imaging in these notes, but these tools are useful for analyzing all imaging modalities.

4.1 Review of useful concepts

4.1.1 Central-limit theorem

4.1.2 Gaussian random variable

4.1.3 Poisson statistics

4.1.4 Stationarity

4.1.5 Ergodicity

4.1.6 Ensemble average

4.2 Resolution

4.2.1 Signal transfer / linear system model

4.3 Noise

4.3.1 Noise transfer (autocorrelation, NPS)

4.4 Contrast

4.4.1 Rose Model

4.5 The effect of Scatter

4.5.1 Resolution: Scatter psf

4.5.2 Contrast: Rose Model

The derivation of expressions for contrast and SNR under the Rose model in section 2.2 neglected the effects of scattered radiation. In general, scattered radiation always works to decrease the contrast and overall quality of an image, as seen in Figure 10. This effect can be quantitatively demonstrated with a simple extension of the Rose model.

Recall our previous definition of contrast under the Rose model,

$$C = \frac{\Delta\phi}{\bar{\phi}} = \frac{\phi_1 - \phi_2}{(\phi_1 + \phi_2)/2} \tag{4.1}$$

Referring to Figure 11, we can define a "no scatter" contrast, C_{NS}, accounting only for contrast from the primary fluence components, ϕ_{1p} and ϕ_{2p}, That is,

$$C_{NS} = \frac{\phi_{1p} - \phi_{2p}}{(\phi_{1p} + \phi_{2p})/2} = \frac{\phi_{1p} - \phi_{2p}}{P} \tag{4.2}$$

where we define P as the mean primary fluence, $(\phi_{1p} + \phi_{2p})/2$.

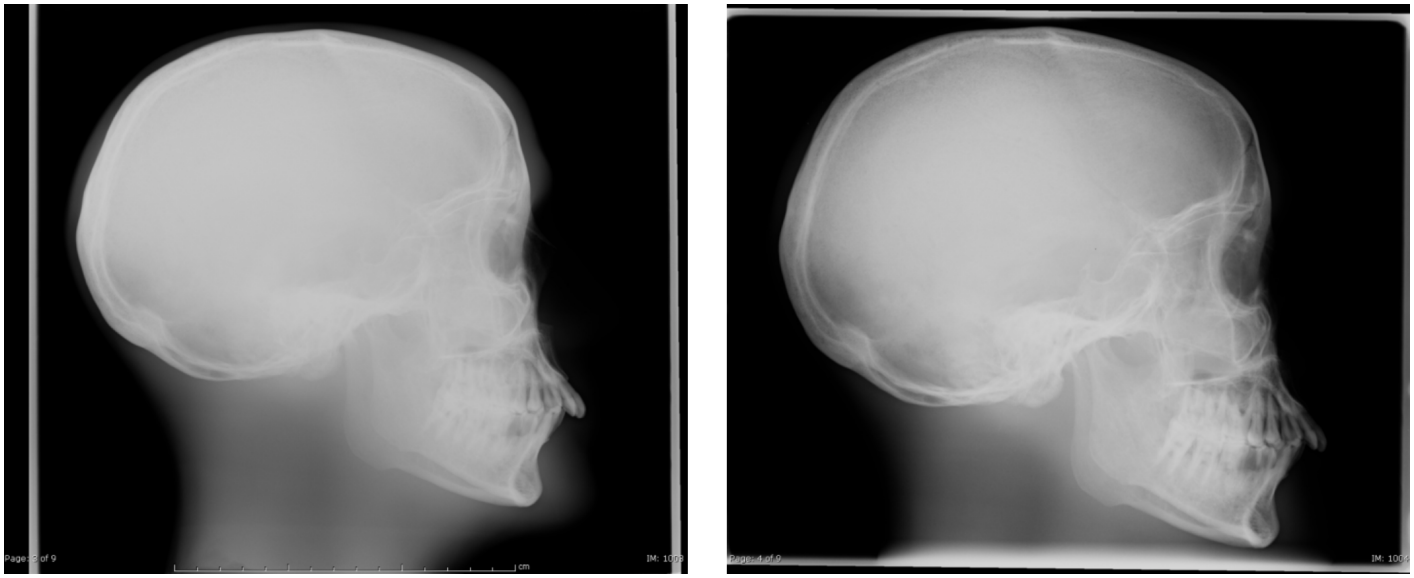

Figure 10: Left: Radiograph of the skull with contrast. Right: Radiograph of the same skull with an anti-scatter grid in place. Note the improvement in image contrast.

Likewise, we can define a "scatter" contrast, C_S,

$$C_S = \frac{(\phi_{1p} + \phi_{1s}) - (\phi_{2p} + \phi_{2s})}{[(\phi_{1p} + \phi_{1s}) + (\phi_{2p} + \phi_{2s})]/2} \tag{4.3}$$

$$= \frac{(\phi_{1p} - \phi_{2p}) + (\phi_{1s} - \phi_{2s})}{[(\phi_{1p} + \phi_{2p}) + (\phi_{1s} + \phi_{2s})]/2} \tag{4.4}$$

$$\tag{4.5}$$

If we assume that the scatter component of each fluence is roughly equal, that is $\phi_{1s} \approx \phi_{2s} = \phi_S$, and define $S = \phi_S$, then C_S can be written

$$C_S = \frac{\phi_{1p} - \phi_{2p}}{P + S} \tag{4.6}$$

and we see that scatter reduces contrast.

We can relate the scatter and no-scatter contrasts as follows:

$$C_S = \frac{\phi_{1p} - \phi_{2p}}{P + S} \left(\frac{P}{P}\right) \tag{4.7}$$

$$= C_{NS} \left(\frac{P}{P + S}\right) \tag{4.8}$$

$$= C_{NS} \left(1 - \frac{S}{P + S}\right) \tag{4.9}$$

$$= C_{NS}(1 - \mathrm{SF}) = C_{NS} \left(\frac{1}{1 + S/P}\right) \tag{4.10}$$

using the scatter fraction:

$$\mathrm{SF} = \frac{S}{P + S} \tag{4.11}$$

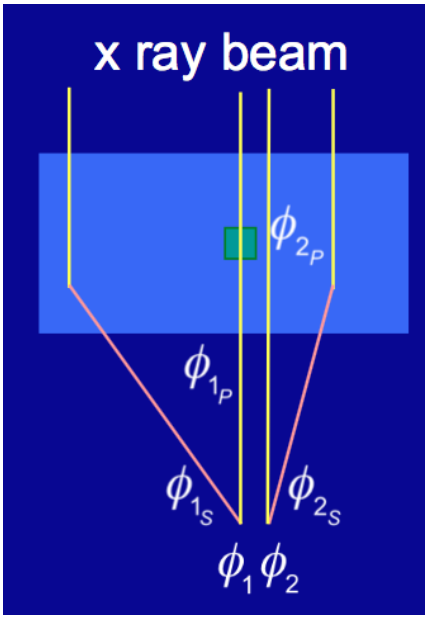

Figure 11: Rose model with scatter.

and scatter-to-primary ratio, S/P.

4.5.3 Anti-scatter grids

5 Image Interpretation

5.1 Six levels of Efficacy

5.2 The Ideal Observer

5.3 Mathematical Observers

5.3.1 Pre-whitening filter

5.3.2 Matched filter

5.3.3 Wiener filter

5.4 Human observers

5.5 Model observers

6 Conclusion

References

[1] Harrison H. Barrett and William Swindell. *Radiological imaging : the theory of image formation, detection, and processing*. Academic Press, New York, 1981. https://doi.org/10.1016/c2009-0-02376-9.

[2] https://chemistry.stackexchange.com/a/59925, 2016. [Online; accessed 11-April-2018].